

# A Squeeze Film Flow Processibility Tester

HOANG T. PHAM<sup>1,\*</sup> and EBERHARD A. MEINECKE<sup>2</sup>

<sup>1</sup>The Dow Chemical Company, Freeport, Texas 77541; <sup>2</sup>Department of Polymer Science, The University of Akron, Akron, Ohio 44325

## SYNOPSIS

The applicability of the squeeze film flow geometry in a processibility tester is investigated in this study. A prototype processibility tester has been built by retrofitting it to a servo-hydraulic load frame. Several processibility parameters such as viscosity and the elastic component in the melt have been investigated. With the concept of equivalent elastic strain, the extrudate swell can be semi-quantitatively predicted from the squeeze film flow experiment. © 1994 John Wiley & Sons, Inc.

## INTRODUCTION

Various polymer processing operations can be simulated by squeeze film flow experiments. One of the simplest analogies is compression molding. In compression molding, polymeric material is placed in a mold and compressed to assume the shape of the mold. Similarly, in squeeze film flow, a polymeric material is placed between two parallel plates and is then squeezed into a thin film. Other simulations may include the pressing of ink-containing polymer additives onto a textile, the flow field in a flat mold of an injection molding process, and blown film extrusion where biaxial extensional flow dominates, and so on.

Squeeze film flow has been proposed by many researchers as a geometry suitable for processibility testing. Leider and Bird<sup>1</sup> used it to determine the power-law constants. Other squeeze film processibility testers such as the Williams parallel plate plastimeter<sup>2</sup> and the Wallace plastimeter<sup>3</sup> have been commercialized. However, these processibility testers do not yield quantitative data. Dienes and Klemm<sup>4</sup> studied the effect of temperature on the viscosity of polyethylene and vinyl chloride acetate resin compounds using squeeze film flow experiments. Shaw<sup>5</sup> used the squeeze film geometry to determine the weight average molecular weight of various polyethylene resins. Pham and Meinecke<sup>6</sup>

proposed a method to determine a power-law characteristic flow curve using constant speed squeeze film flow experiments. They observed good agreement between the data obtained from squeeze film flow and capillary rheometry experiments for natural rubber compounds, (SMR 5), ethylene propylene rubber (EPDM), and a styrene butadiene styrene copolymer (Kraton).

The objective of this study is to evaluate the feasibility of the squeeze film flow geometry for the design of a processibility tester. A prototype processibility tester has been built, and the processibility parameters such as viscosity, the elastic component of the polymer's response to a given deformation, and so on, have been investigated. Furthermore, using the squeeze film flow apparatus, the effects of processing time on the viscosity of natural rubber and of carbon black loading on that of EPDM was studied. A proposed concept of equivalent elastic strain is introduced to qualitatively predict extrudate swell from squeeze film flow experiments.

## THEORY

### Mechanism of Squeeze Film Flow

A polymer melt is placed between two flat parallel plates. The plates are at rest for  $t < 0$ . At time  $t = 0$ , the plates are activated to move toward each other at a constant speed,  $\dot{h}$ . Immediately after movement has started, no flow will occur. The melt is under-

\* To whom correspondence should be addressed.

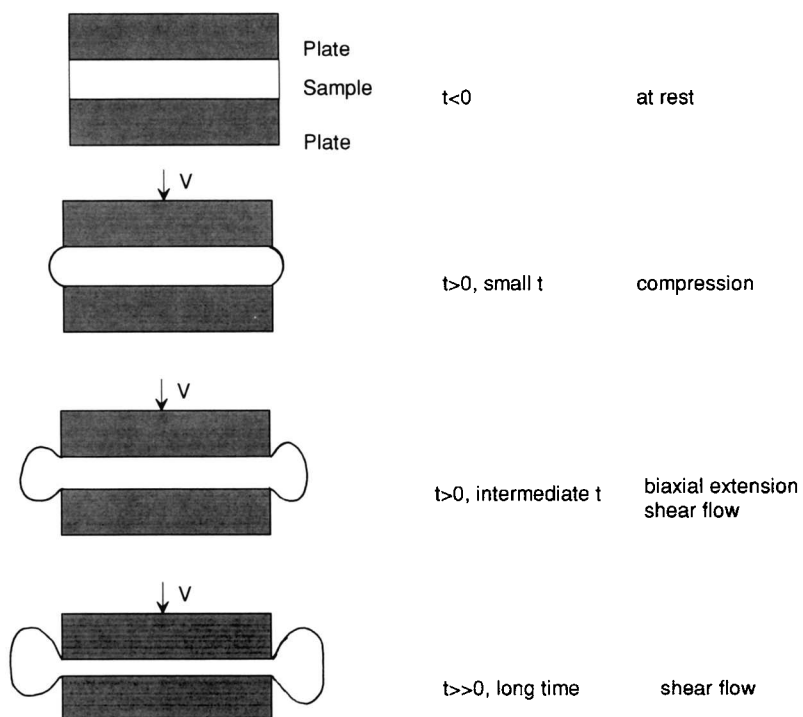


Figure 1 Mechanism of squeeze film flow.

going compression just as a bonded rubber block would. As the plate continues to move, viscous flow will take place and the melt will undergo shear deformation at the solid–fluid interfaces and biaxial

extensional flow in the center region. Only after long squeezing times, when the radius to gap height ratio ( $R/h$ ) is large,<sup>4</sup> will the melt undergo predominantly shear flow. This mechanism is illustrated in Figure 1.

	NATURAL RUBBER (SM R5)		EPDM 2504	KRATON 3204
	CV60	CV102		
Develop & Design		Mechanical Breakdown	Thermally stable, Negligible breakdown under mechanical shear	
		Various Masticating time (0 - 12 min.)	Various carbon black (N550) loading (0 - 30 phr)	
<b>Recipe</b>				
Rubber	-	100 phr	100 phr	100 phr
N990	-	40 phr	0 phr	0 phr
N550	-	40 phr	Variable	0 phr
Processing aids	-	5 phr Sunpar	0.7 phr Flexol 815	0 phr
Mixing	-	-	Internal Mixer (150 °C discharge temperature)	-
Milling	-	Variable	6 min.	-
Shaping	3 min. on open mill	3 min. on open mill	compression molding (50 tons/10" ramp)	compression molding (65 tons/10" ramp)
Sampling	Direct from milled sheets	Cylindrical disks (R=3.81 cm, h <sub>0</sub> =0.975 cm) Direct from milled sheets	Cylindrical disks (R=3.81 & 2.54 cm, h <sub>0</sub> =0.993 cm) From molded sheets	Cylindrical disks (R=3.81 cm, h <sub>0</sub> =0.977 cm) From molded sheets

Figure 2 Experimental scheme flow chart including materials and their preparations.

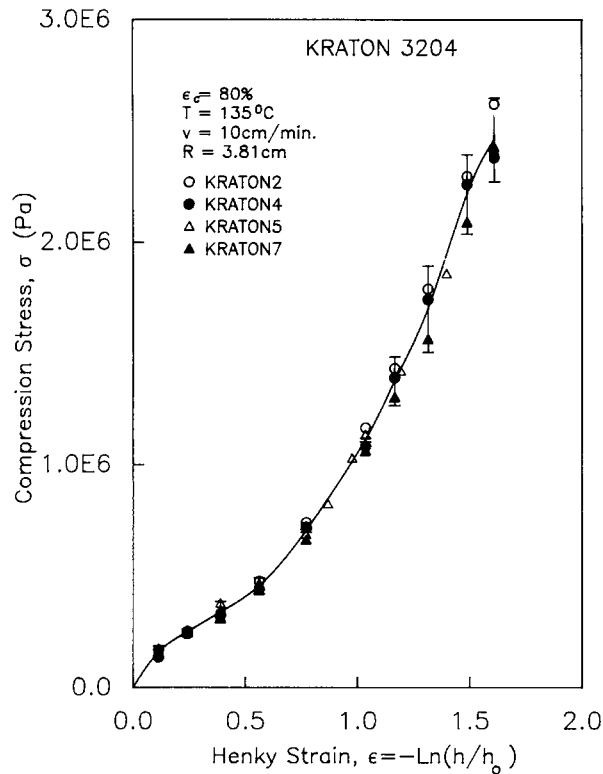


**Figure 3** Compression stress versus henky strain for kraton 3204 samples tested under identical conditions.

### The Concept of Equivalent Elastic Strain

Polymer melts are viscoelastic, that is, their behaviors consist of a viscous and an elastic response to an applied deformation. The simplest way to represent this behavior is with the help of a Maxwell

model, namely, a spring and a dash pot connected in series. The spring represents the elastic contribution and is characterized by a shear modulus  $G$  and an elastic strain  $\gamma_e$  that is reversible. The dash pot represents the viscous contribution and is characterized by an arbitrary viscosity,  $\eta$ , which can be a function of the shear rate  $\dot{\gamma}$  and the viscous shear strain,  $\gamma_v$ , which is irreversible.

As the melt is being sheared, the total shear strain can be written as follows:

$$\gamma_t = \gamma_e + \gamma_v \quad (1)$$

At a given shear strain, the shear stress is the same in both parts comprising the model, so that

$$\tau_{12} = \tau_{12,e} = \tau_{12,v} \quad (2)$$

where  $\tau_{12,e}$  is the shear stress placed on the spring, that is, the elastic shear stress, and  $\tau_{12,v}$  is the shear stress placed on the dash-pot, that is, the viscous shear stress.

The elastic and the viscous shear stresses can be written as

$$\tau_{12,e} = G\gamma_e h(\gamma_e) \quad (3)$$

and

$$\tau_{12,v} = \eta(\dot{\gamma})\dot{\gamma} \quad (4)$$

where  $h(\gamma_e)$  is a nonlinear damping function that depends only on  $\gamma_e$  for the nonlinear spring and  $\dot{\gamma}$

**Table I** Loading Curve Data for Kraton 3204 Tested Under Identical Conditions

Time (sec)	Gap Height (cm)	Loading Stress (MPa)					Average	Std. Dev.
		Kraton 2	Kraton 4	Kraton 5	Kraton 7			
0.25	0.872	0.17	0.14	0.17	0.16	0.16	0.014	
0.5	0.767	0.25	0.24	0.26	0.25	0.25	0.006	
0.75	0.662	0.33	0.33	0.38	0.32	0.34	0.024	
1.0	0.557	0.48	0.44	0.47	0.44	0.46	0.018	
1.25	0.452	0.74	0.72	0.69	0.66	0.70	0.030	
1.5	0.347	1.17	1.08	1.14	1.06	1.11	0.042	
1.6	0.305	1.43	1.39	—	1.30	1.38	0.055	
1.7	0.263	1.79	1.74	—	1.57	1.70	0.097	
1.8	0.221	2.29	2.26	—	2.09	2.22	0.089	
1.86	0.195	2.62	2.38	2.41	2.43	2.46	0.095	

Note.: Testing conditions: temperature = 135°C; Plate velocity = 10 cm/min; Sample and plate radius = 3.81 cm; Initial Gap = 0.977 cm; Compression Strain = 80%.

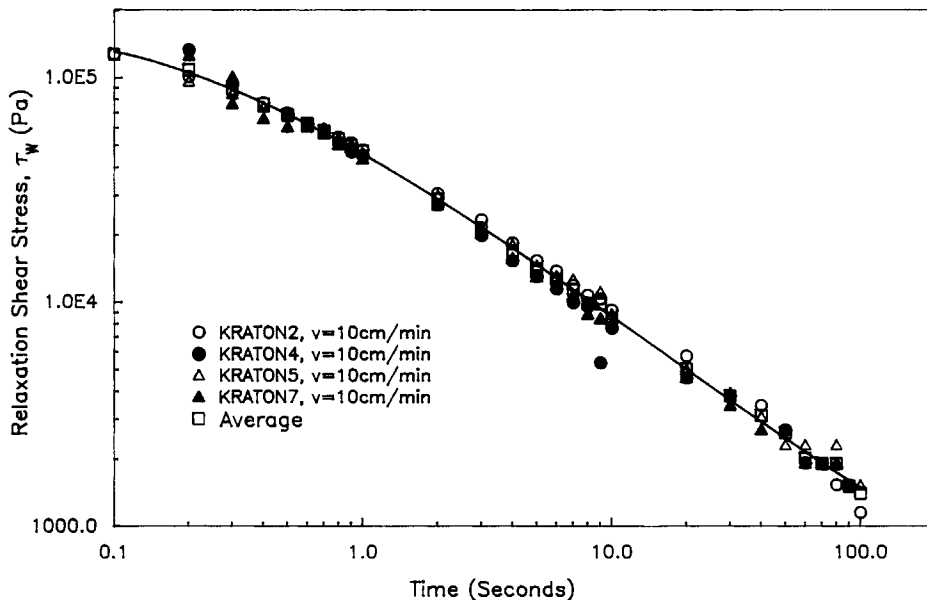


**Figure 4** Relaxation shear stress as a function of time for various Kraton 3204 samples tested under identical conditions.

is the rate of shear deformation. Then the following expression is obtained from eq. (2):

$$G\gamma_e h(\dot{\gamma}) = h(\dot{\gamma})\dot{\gamma} = \tau_{12,v} = \tau_{12} \quad (5)$$

The equivalent elastic strain is defined as

$$\gamma_r = \|\gamma_e h(\dot{\gamma})\| \quad (6)$$

where  $\|\gamma_e h(\dot{\gamma})\|$  is the magnitude of the elastic strain tensor,  $\gamma_e$ , multiplied by the nonlinear damping function,  $h(\dot{\gamma})$ . Thus,

$$\gamma_r = \frac{\|\tau_{12}\|}{G} \quad (7)$$

### The Shear Modulus

The shear modulus can be determined in the compression region, that is, for short times after the

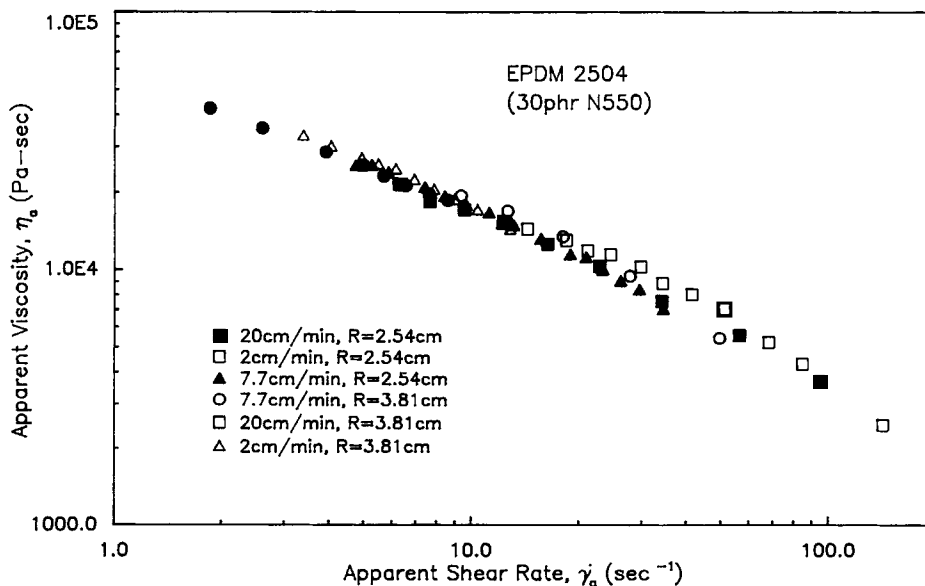


**Figure 5** Apparent viscosity as a function of apparent shear rates for EPDM 2504 containing 30 phr of N550, tested at various squeeze film flow experimental conditions.

**Table II Viscosity Level Scattering in Squeeze Film Flow Experiments at All Testing Conditions**

Material	Batch ID	No. of Samples	% Scattering
SMR5-CV60	NRA1	6	11
SMR5-CV102	NRA2	4	4.7
	NRB	2	< 1
	NRC1	2	< 1
	NRC2	2	4.3
	NRC3	2	3.1
	NRC7	2	1.1
	EPDM 2504	Gum	6
	0.25 phr	3	2.5
	10 phr	4	16
	30 phr	9	5.3
Kraton 3204	Kraton	6	4.6

plates have started to approach each other. Assuming that the bulk modulus is very high, then by applying the bonded block theory<sup>7,8</sup> an extension modulus  $E$  can be determined by

$$E_{app} = E(1 + 2s^2) \tag{8}$$

where  $E_{app}$  is the apparent modulus measured in compression,  $s$  the shape factor. For cylindrical disks, the shape factor is  $s = R/4h_0$ , with  $R$  the radius of the disk and  $2h_0$  its thickness. For an in-

compressible fluid, the relationship between the shear modulus and the extension modulus is given by

$$G = \frac{1}{3}E \tag{9}$$

**EXPERIMENTAL**

The squeeze film flow experiment was set up by retrofitting a servo hydraulic multitester manufactured by CGS Scientific Corporation, model 109. The squeeze film flow apparatus consisted of two cylindrical blocks with a radius of 5.08 cm (2 in). Each block consisted of three sections. The section that connects to the load frame of the multi-tester was made of a 1020 low carbon steel. The middle section was made of a machinable ceramic material 2.54 cm (1 in) thick. It functioned as a thermal insulator. The last section was an aluminum piece with a recessed melt contacting surface with a radius of 3.81 cm (1.5 in). This recess was provided so that the melt could be heated uniformly by having the band heaters pulled down over the recessed area during the heating stage. An adapter with a radius of 2.54 cm was used to perform tests on the samples with a smaller diameter.

The test fixture was heated by two band heaters, each controlled by an Omega RTD temperature

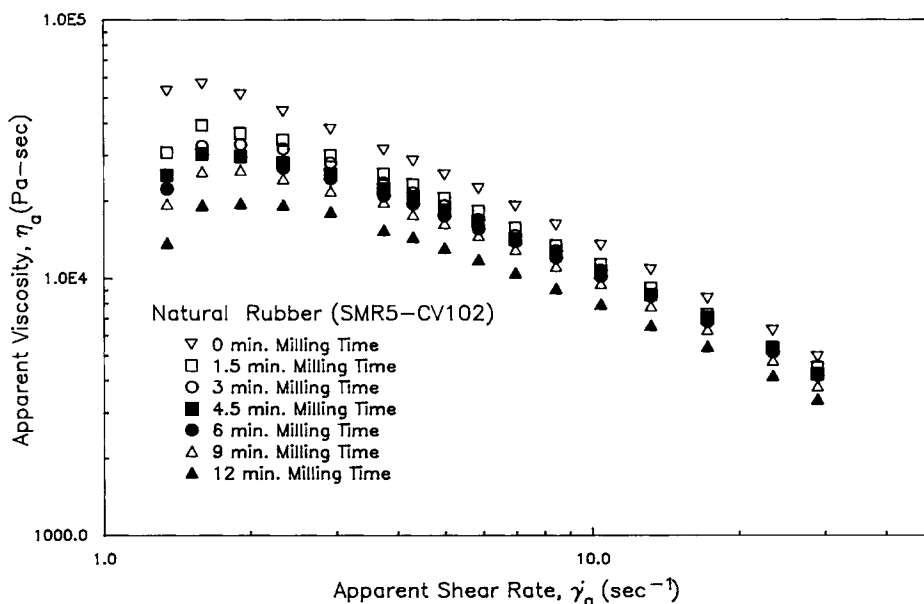


**Figure 6** Effect of masticating time on the apparent viscosity as a function of apparent shear rates for SMR5-CV102.

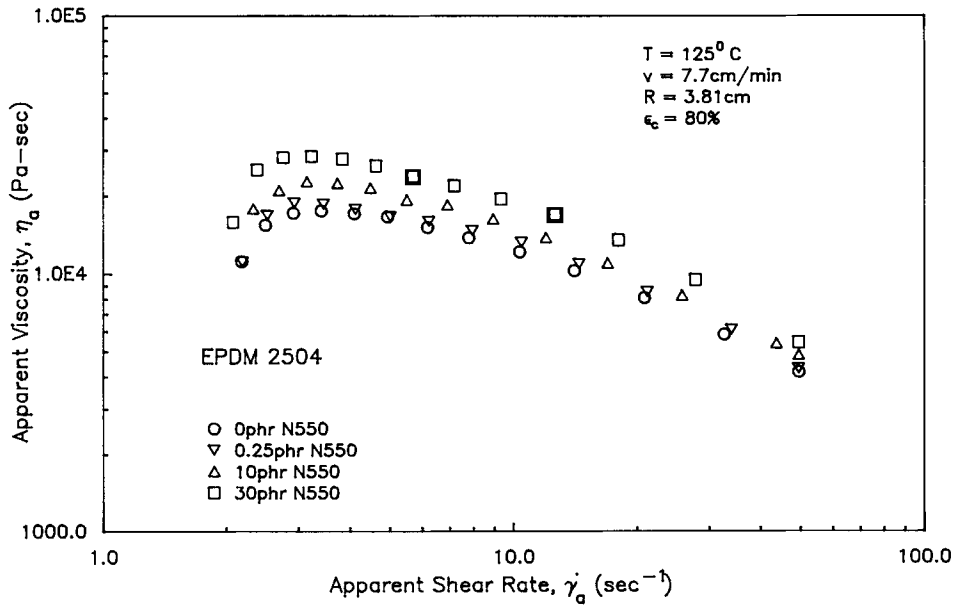


**Figure 7** Effect of carbon black loading on the apparent viscosity as a function of apparent shear rates for EPDM 2504 (7.7 cm/min plate velocity).

controller. A polymeric sample having a cylindrical disk shape was placed between the plates and heated to the testing temperature. The time required to reach equilibrium temperature was established by

calibration curves for a given shape (sample thickness). After the melt temperature had been reached, the lower plate was made to move towards the upper one at constant speed. The movement was stopped

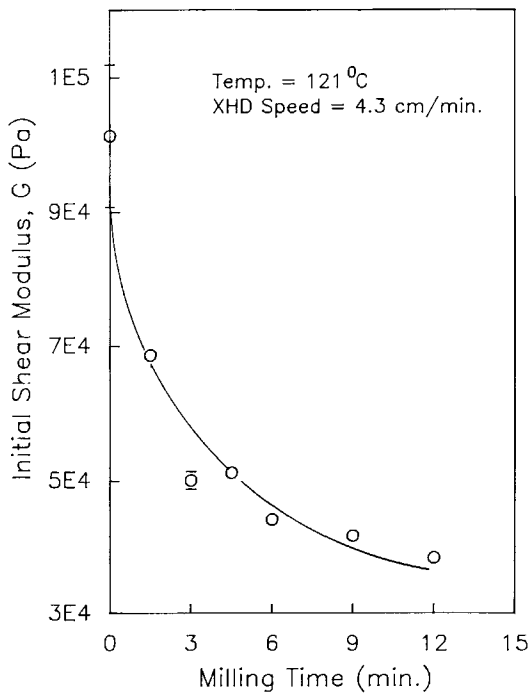


**Figure 8** Initial shear modulus as a function of milling time for SMR5-CV102.

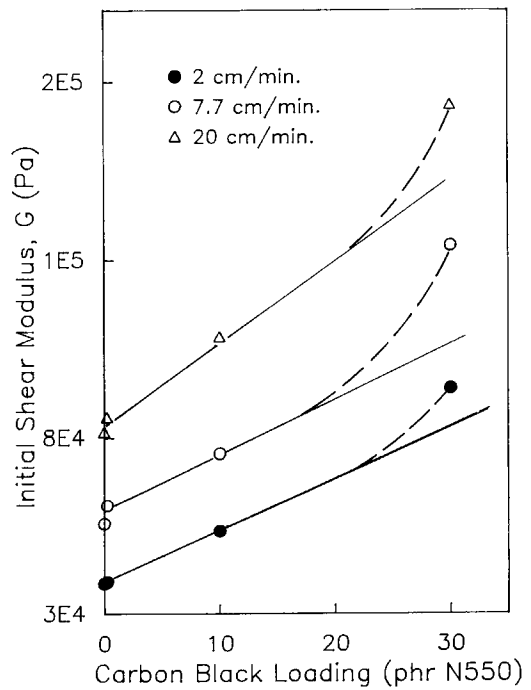


**Figure 9** Initial shear modulus as a function of carbon black loading for EPDM 2504.

**Table III Comparison of the Initial Shear Modulus as a Function of Carbon Black Loading with Predictive Theories**

EPDM 2504 phr N550 (by Weight)	Volume Fraction $\phi$	Effective Volume Fraction $\phi'$	EGG Prediction G (Pa)	MEGG Prediction G (Pa)	Experimental G (Pa)
0	—	—	—	—	55,000
0.25	0.0011	0.0027	55,200	55,400	61,000
10	0.044	0.1085	62,600	79,100	75,600
30	0.122	0.3013	83,300	166,800	134,000

Note: Equation:  $P = P_0(1 + 2.5\phi + 14.1\phi^2)$ .  $\phi$  = volume fraction (Einstein Guth Gold - EGG).<sup>9</sup>  $\phi' = \phi$  = effective volume fraction (Medalia's correction - MEGG).<sup>10</sup>

after the plates had approached each other to a given compression strain. The load and distance traveled were monitored and recorded onto a floppy disk via an analog/digital converter (Metrabyte Dash-16) and a wave form scroller card (WFS-200 by Dataq).

Experiments were performed on natural rubber compounds (SMR5-CV102) milled for various amounts of time to study the effect of processing time. Natural rubber was chosen since it breaks down under mechanical shear, that is, its molecular weight decreases.<sup>9</sup> An ethylene propylene rubber (EPDM Vistalon 2504) was used to study the effect of carbon black (N550) loading. A styrene-butadiene-styrene copolymer (Kraton 3204) was also tested. Figure 2 shows the experimental scheme used in this study.

## RESULTS AND DISCUSSION

The reproducibility of the experiments was analyzed using three types of data analyses. First, the reproducibility of the load-deflection curve shown in Figure 3 for Kraton 3204 and the data scattering was tabulated in Table I. For all samples tested, the scatter was found to be within 10%. Second, the stress relaxation after cessation of squeezing action was also analyzed, as shown in Figure 4 for Kraton 3204. Data scattering was found to be within 10% for samples tested under identical experimental conditions. Third, the reproducibility of the viscosity data, determined according to the method proposed by Pham and Meinecke<sup>6</sup> was analyzed. The result is shown in Figure 5 for EPDM containing 30 phr N550 carbon black tested at various squeezing speeds. Table II tabulates the scatter of the viscosity data for some of the samples tested under various experimental conditions. Scatter is less than 10% except for the natural rubber compound (SMR5-

CV60) and EPDM containing 10 phr N550 carbon black.

The apparent viscosity as a function of apparent shear rate for natural rubber compounds (SMR5-CV102) milled for various times is depicted in Figure 6. As the milling time increases, natural rubber breaks down due to mechanical shear which reduces the viscosity. This trend is detected by the squeeze film flow experiments. Figure 7 illustrates the effect of carbon black loading of EPDM rubber. The squeeze film data show the trend established by previous studies,<sup>11,12</sup> that increasing carbon black loading increases the viscosity. These effects, namely,

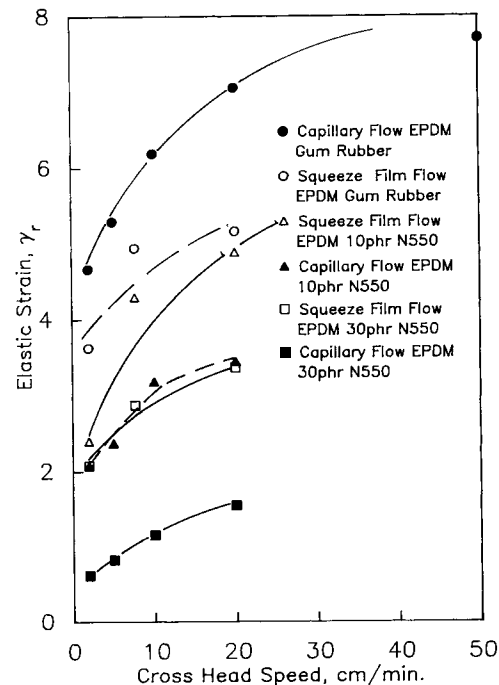


**Figure 10** Elastic strain as a function of cross head speeds for EPDM 2504.

**Table IV** Equivalent Elastic Strain and Extrudate Swell Ratio as a Function of Cross Head Speed for EPDM Compounds and Kraton

Cross Head <sup>a</sup> Speed (cm/min)	EPDM 2504						Kraton 3204	
	0 phr		10 phr		30 phr		$\gamma_r$	$B_\infty$
	$\gamma_r$	$B_\infty$	$\gamma_r$	$B_\infty$	$\gamma_r$	$B_\infty$		
2	3.62	1.61	2.39	1.31	2.07	1.13	2.89	1.25
5	—	1.67	—	1.34	—	1.15	—	—
7.7	4.83	—	4.29	—	2.84	—	—	—
10	—	1.75	—	1.45	—	1.19	3.38	1.25
20	5.16	1.81	4.88	1.48	3.36	1.24	3.49	1.25
50	—	1.88 <sup>b</sup>	—	1.45 <sup>b</sup>	—	1.24	—	1.25

<sup>a</sup> Squeeze film flow speeds are the plate velocity.

<sup>b</sup> Surface distortion observed on extrudates.

the processing time of natural rubber and carbon black loading of EPDM rubber, are clearly seen in the initial shear modulus as shown in Figures 8 and 9. The nonlinear increase in the initial shear modulus with increasing carbon black loading is found to agree with the modified Einstein-Guth-Gold equation.<sup>13</sup> The prediction and experimental initial shear moduli are compared in Table III.

Another well-known processibility parameter is extrudate swell,  $B_\infty$ . *Extrudate swell* is defined as the ratio of the extrudate diameter to the die diameter. Extrudate swell is due to the "elastic memory" left in the melt after exiting the die.<sup>14</sup> Peng<sup>15</sup> have shown that extrudate swell can be described by an "elastic memory" quantity called the *elastic recoverable strain*. Similarly, the equivalent elastic strain as defined by eq. (7) is used in this study to qualitatively predict extrudate swell. This is illustrated in Figure 10 and tabulated in Table IV. The equivalent elastic strain is found to increase with increasing squeezing speed in the same manner as the elastic recoverable strain derived from capillary rheometry. In Figure 10, the elastic strains derived from capillary and squeeze film flow experiments are plotted against cross head speed. The cross head speed is used here for comparison instead of the shear rate because of the difficulty to define a single shear rate for the squeeze film flow. This difficulty arises because the rate of shear deformation changes throughout the whole experimental run. In addition, the equivalent elastic strain increases with increasing carbon black loading as observed from capillary extrusion experiments. Thus, extrudate swell can be qualitatively predicted by comparing the trends of the equivalent elastic strain obtained from squeeze film flow experiments.

## CONCLUSIONS

A prototype squeeze film flow apparatus has been built and used to determine the rheological properties of polymer melts. This investigation showed that this is feasible to use the squeeze flow geometry under constant strain rate conditions for processibility testing. The squeeze film flow apparatus can quantitatively predict the viscosity as proposed by Pham and Meinecke<sup>6</sup> and can also predict quantitatively elastic effects. Furthermore, the usefulness of squeeze film flow has been demonstrated by the study of the effect of processing time of natural rubber compounds and the effect of carbon black loading of EPDM rubber. The trends of these effects found by squeeze film flow agree with previous studies. In addition, extrudate swell can be qualitatively predicted by squeeze film flow experiments via the equivalent elastic strain parameter.

Financial support of this research by the Edison Polymer Innovation Corporation (EPIC) is gratefully acknowledged.

## REFERENCES

1. P. J. Leider and R. B. Bird, *Ind. Chem. Eng.*, **13**(4) (1974).
2. R. W. Wise, *Rubber Technology*, M. Morton, Ed., 2nd ed., R. E. Kreiger Pub. Co., Malabar, FL, (1981).
3. A. N. Gent, *British J. Appl. Physics*, **11**, 85 (1960).
4. G. J. Dienes and H. F. Klemm, *J. Appl. Physics*, **17**, 458 (1946).
5. M. T. Shaw, *Polym. Eng. Sci.*, **17**, 266 (1977).



6. H. T. Pham and E. A. Meinecke, *J. Appl. Polym. Sci.*, **53**, 257 (1994).
7. A. N. Gent and P. B. Lindley, *Proc. Inst. Mech. Eng. (G. Britain)*, **173**(3), 111 (1959).
8. A. N. Gent and E. A. Meinecke, *Polym. Eng. Sci.*, **10**, 48 (1970).
9. G. O. Bristow and W. F. Watson, *Chemistry and Physics of Rubber Like Substances*, L. Bateman, Ed., John Wiley Intersci., NY, 1963.
10. C. C. McCabe, in *Reinforcement of Elastomer*, G. Kraus, Ed., Wiley, NY, 1965, Chap. 7, pp. 225–245.
11. E. Guth, *Rubber Chem. Tech.*, **8**, 596 (1945).
12. E. A. Meinecke and M. I. Taftaf, *Rubber Chem. Tech.*, **61**, 534 (1988).
13. A. I. Medalia, *Rubber Chem. Tech.*, **51**, 437 (1978).
14. R. I. Tanner, *J. Polym. Sci.*, **A8**, 2067 (1970).
15. L. Peng, PhD Dissertation, 1991, University of Akron.

Received September 3, 1993

Accepted January 10, 1994